THE EFFECT OF TRACE ADDITIONS ON THE PRECIPITATION MICROSTRUCTURE OF AN Al-4.1Cu-1.6Mg ALLOY

L.M. RYLANDS, W.M. RAINFORTH and H. JONES

Department of Engineering Materials, University of Sheffield, Mappin Street, Sheffield, S1 3JD, UK

ABSTRACT Small additions of indium, silicon, lanthanum, and further magnesium were made to an Al-4.1Cu-1.6Mg alloy. Specimens were solutionised and then aged for 100h at 200°C and the resulting microstructures examined using TEM and compared with that of the base alloy with no additions. Precipitate size measurements were taken for S' from aged specimens. In addition, Vickers hardness tests were carried out on the aged specimens and compared to results for the Al-4.1Cu-1.6Mg base alloy. The distribution of the S' precipitates in all of the alloys containing additions was more non-uniform than in the base Al-4.1Cu-1.6Mg alloy. In the alloys containing additions, the stability of the GPB zones appeared to be increased compared to the base alloy. The mean S' precipitate particle volume was significantly larger in the alloys containing additions, as was the mean length of S' corrugations. The hardness of the specimens after 100h ageing varied depending on the addition used, with the alloy containing extra magnesium having the highest hardness value after ageing.

Keywords: *Al-Cu-Mg, trace elements, ageing, microstructure, hardness.*

1. INTRODUCTION

Limited work has been undertaken on the effect of trace additions on the age hardening behaviour of aluminium alloys [1-6]. Furthermore, the majority of these have concentrated on short ageing times, particularly around peak hardness. Our previous work [7-9] has demonstrated that, for times up to 10,000h at 200°C, alloys hardened by S' exhibit good strength when compared to other Al-alloys hardened by a single precipitate type (i.e. Ω, θ', δ' or β'). High resolution TEM (HREM) investigations [7,10] have indicated that the coarsening of S' occurs by a ledge-growth mechanism. Therefore, a reduction in ledge migration rate should reduce coarsening rate of the precipitate and therefore provide superior temperature stability of the alloy. Added solute atoms of size larger than that of Al and with low solubility in the aluminium matrix, should segregate to the precipitate/matrix interface and thus inhibit ledge migration. In the current study, trace La, In, Si, and extra Mg were added to an Al-4.1Cu-1.6Mg base alloy to determine their effect on the precipitate structure and the hardening characteristics. An ageing time of 100h at 200°C was selected since this is in the steady state coarsening regime for the base Al-4.1Cu-1.6Mg base alloy [7].

The level of trace addition to the Al-Cu-Mg base alloy was chosen as that which would provide at least one atom layer coverage of all ledge sites on S′ precipitates. High-resolution TEM images [7] indicated an average ledge height of 0.34nm, with an average of 12 ledges along each precipitate. Table 1 gives the required minimum level of each addition based on the average precipitate volume measured for the base alloy aged for 200°C for 100h (the full details of this calculation are given in ref. [11]).

2. EXPERIMENTAL

The procedures were as reported previously [5]. A base alloy of composition Al-4.1Cu-1.6 Mg-0.1Mn was vacuum melted from 99.99wt% pure feedstock materials. Trace additions were made to

3kg melts to give the alloy compositions detailed in Table 2. All match or exceed the required minimum levels indicated in Table 1. The cast ingots of 76mm diameter were preheated to 300°C for 1h prior to extrusion to rectangular cross-sectioned bar at an extrusion ratio of 10:1. 1cm^3 samples were solutionised at 495°C for 4h before quenching into cold water and immediately ageing at 200°C for 100h. Specimens were electrothinned for TEM and precipitate size measurements were made from the TEM negatives. Typically between 40 and 200 precipitates were measured for each alloy to obtain the average values of length *l*, thickness *t* and width *w* of the precipitate, where these values refer to the size of an individual S' lath in a corrugation containing several S' laths (see Fig. 1). In addition, the total corrugation length, *y*, was measured, also defined in Fig. 1.

3. RESULTS

The microstructure of the base alloy was described in detail elsewhere [11]. The high aspect ratio S′ laths, viewed with the long axis end-on for a beam direction of $[001]_{Al}$, Fig. 1, were present as a distinctive 'corrugated structure'. Each corrugation consisted of several individual laths immediately adjacent or in contact, but with alternate laths adopting a different orientation with the matrix along the precipitate short dimensions. The corrugations in the base alloy were evenly distributed, with average lath dimensions given in Table 3 and average corrugation length, *y*, given in Table 4.

The trace additions all modified the size and morphology of the S′ laths and corrugations. An increase in the Mg content led to a more heterogeneous distribution of the S′ laths and corrugations, such that locally high densities of S′ were present in some regions while others, such as in Fig. 2, were largely free of S′. S′ laths viewed edge-on were arranged in loops, presumably as a result of precipitation on dislocations during the early stages of ageing. Tables 3 and 4 show that the average dimension of the individual laths and of the corrugations was substantially larger than in the base alloy. Fig. 2 shows that a fine dispersion of GPB zones were resolvable in bright field images at moderate magnifications, although GPB-free zones existed adjacent to the S′ laths.

Fig. 3 shows that the distribution of S′ was relatively uniform in the Al-Cu-Mg-In alloy, similar to that found in the base alloy. GPB zones were present in most areas of the foil, although they were difficult to image because of substantial strain contrast associated with the S′/matrix interface. GPB zone size was comparable to the Mg-rich alloy, although the volume fraction was visibly lower. The average volume of individual laths and the length of the corrugations was about twice that of the base alloy, as shown in Tables 3and 4.

Figure 4 shows that the addition of La also promoted a more heterogeneous distribution of the S′ corrugations. Interestingly, a criss-cross arrangement of the S′ precipitates was found, not present in the base alloy. Substantial strain contrast was associated with the S′/matrix interface. The precipitate volume and corrugation length (Tables 3 and 4) were substantially larger than in the base alloy, although not as large as in the Mg-rich alloy. Fine GPB zones were present in localised areas in a manner similar to the Al-Cu-Mg-In alloy.

Fig. 5 shows that the distribution of the S′ in the Al-Cu-Mg-Si alloy was the most uniform of the microstructures of the alloys containing trace additions Nevertheless, the added Si had promoted significant increases in precipitate and corrugation dimensions (Tables 3 and 4) compared to the base alloy. A fine dispersion of GPB zones was also present.

The hardness of all alloys aged for 100h at 200°C is given in Table 5. Compared to the base alloy, added Mg increased the hardness, In had no effect, while Si and La both decreased it.

4. DISCUSSION

In all alloys the main precipitate phase was S′, largely present in corrugations containing several S′ laths. The distribution of the corrugations was significantly more heterogeneous for the

alloys containing trace additions, compared to the alloy without addition. This is in agreement with the findings of Zheng *et al.* [12] who added 0.05% La to an Al-Li-Cu-Mg-Zr alloy (AA8090), and also observed an increase in size of the S′. The reason for this non-uniformity may be because the additional elements had themselves already segregated and hence only had localised effects on S′ precipitation. This point could not be verified since the levels of indium, lanthanum and silicon were too low to detect by EDS analysis in a conventional TEM. However, it is well known that S′ nucleates heterogenously on residual dislocations, and therefore the precipitate distribution partly reflects the prior dislocation distribution. It is possible, therefore, the principal effect of the trace additions was on the active dislocation density and distribution prior to precipitate nucleation.

The GPB zones observed in the present work are similar to those reported by Silcock [13]. In the base alloy, GPB zones were only observed in bright field TEM images of samples aged for short times, but had dissolved during ageing for 100h at 200°C [12]. Although a rigorous analysis was not carried out (this would have required extensive HREM), the diameter of the GPB zones in the alloys with trace additions was typically ~7nm. This compares with a maximum of ~2nm observed in the base alloy after 10h at 200°C (full details in ref. [11]). This implies that the addition of indium, lanthanum, silicon or extra magnesium increases the stability of GPB zones in Al-4%Cu-1.5%Mg. The effect of silicon in increasing the stability of GPB zones was first reported by Wilson *et al.* [5] who suggested that it may be as a result of silicon incorporated into the GPB structure. However, the effect of indium on precipitation in Al-Cu alloys has been reported as hindering the formation of GP zones at an ageing temperature of 190°C (Silcock [2], Silcock *et al.* [3]), in contrast to the present work where the GPB volume fraction was higher than in the indium free alloy. Silcock *et al.* suggested that indium caused a reduction in the amount of copper available for S′ precipitation by tying it up in clusters with the ternary addition.

The mean volume per precipitate in all the alloys containing trace additions was larger than for the base Al-Cu-Mg alloy (Table 3). It is expected that this would have a deleterious effect on the hardness of the alloys. S′ precipitates are looped rather than sheared by dislocations (Gregson and Flower [14]) and any increase in mean spacing between precipitates at constant volume fraction causes a reduction in the contribution of the precipitates to Orowan hardening. Table 5 indicates that this is the case for the lanthanum and silicon containing alloys which have a significantly lower hardness than the base Al-Cu-Mg alloy. The indium-containing alloy, however, retains the same hardness as the Al-Cu-Mg alloy despite having a mean S′ precipitate volume almost twice that of the plain Al-Cu-Mg alloy. A considerable increase in hardness for the Mg-rich alloy over that of base Al-Cu-Mg alloy aged under the same conditions was observed which is somewhat surprising when the former alloy has a mean volume per S′ precipitate approximately six times larger than the latter. This suggests that the GPB zones in the Mg-rich alloy and the indium containing alloy provide a substantial hardening effect. A contribution to the hardening in the Mg-rich alloy may also be attributed to the solid solution hardening effect of the extra magnesium present.

Further work is required to determine the long term effects of additional elements on the coarsening and hardening behaviour of Al-Cu-Mg alloys. Initial observations indicate that several factors may act to change the coarsening behaviour of alloys containing trace additions. For example, the effect of increased interfacial strain observed at the S′ precipitate/matrix interface could be to increase the driving force for coarsening. HREM observations and microanalysis are required to determine the extent to which the elements added are situated at interfacial ledges and have an effect on coherency at the precipitate/matrix interface.

5. CONCLUSIONS

1. Trace additions of indium, silicon, lanthanum, and further magnesium were made to an Al-4.1Cu-1.6Mg alloy. In all cases, the addition increased the average volume per S′ precipitate, and increased the heterogeneity of the precipitate distribution.

2. All these additions increased the stability of GPB zones compared to the base alloy.
3. Trace additions of La and Si decreased hardness; the hardness of the In alloy was unchanged while the Mg-rich alloy had a higher hardness than the base Al-Cu-Mg alloy.

Acknowledgements

The authors are grateful to the University of Sheffield (Hossein Farmy Scholarship Fund) and to DERA, Farnborough, for providing financial support for this work which formed part of a PhD programme for LMR.

REFERENCES

1. I.J. Polmear, Materials Science Forum, 13/14(1987), 195.
2. J.M. Silcock, J. Inst. Metals, 84(1955-56), 19.
3. J.M. Silcock,, T.J. Neal and H.K Hardy, J. Inst. Metals, 84(1955-56), 23.
4. H.K. Hardy, J. Inst. Metals, 80(1951-52), 483.
5. R.N. Wilson, D.M. Moore and P.J.E. Forsyth, J. Inst. Metals, 95(1965), 177.
6. S. Özbilen and H.M. Flower, Acta Metall., 37(1989), 2993.
7. L.M. Rylands, H. Jones and W. M. Rainforth, in 'Lightweight Alloys for Aerospace Applications', eds. E.W. Lee, N.J. Kim, K.V. Jata and W.E. Frazier, TMS, Warrendale, Pa, 1995, pp 129.
8. L.M. Rylands, D.M.J. Wilkes, W.M. Rainforth and H. Jones, J Mater. Sci., 29(1994), 1895.
9. L.M. Rylands, H. Jones and W. M. Rainforth, Phil. Mag. Lett. 76(1997), 63.
10. V. Radmilovic, G. Thomas, G. Shiflet and E.A. Starke, Scripta Metall., 23(1989), 1141.
11. L.M. Rylands, PhD Thesis, University of Sheffield, 1995.
12. Z.Q. Zheng, Y.Q. Zhao, M.G. Liu and D.F. Yin, J. Mater. Sci. Let., 13(1994), 946.
13. J.M. Silcock, J. Inst. Met., 89(1960-61), 203.
14. P.J. Gregson and H.M. Flower, Acta Metall., 33(1985), 527.

Table 1. Minimum level of addition required achieve one monolayer coverage of the S′ precipitate/matrix ledges in Al-Cu-Mg aged for 100h at 200°C.

Element	Atomic diameter (nm)	Atomic Weight	wt % element required	Eutectic Temp. T_{eu} (°C)	Solubility in α-Al at T_{eu} (wt%)
Mg	0.320	24.31	0.009	450	17.4
Si	0.396	28.09	0.009	577	1.65
In	0.314	114.8	0.046	637	0.15
La	0.374	138.9	0.046	642	0.05

Table 2. Alloy compositions in weight percent

Alloy designation	Cu±0.04	Mg ±0.02	Addition	Level
Al-Cu-Mg	4.11	1.55	None	
Al-Cu-Mg (+Mg)	4.11	2.55	Mg	2.55 ± 0.02
Al-Cu-Mg-In	4.25	1.60	In	0.19 ± 0.02
Al-Cu-Mg-La	4.25	1.56	La	0.043 ± 0.005
Al-Cu-Mg-Si	4.15	1.60	Si	0.18± 0.02

Table 3. Precipitate size data for S′ for specimens aged for 100h at 200°C. n_{ppts} indicates the number of precipitates measured. $\bar{x}$ is the mean measured dimension with one standard deviation.

Alloy Identification		(Al-Cu-Mg)	(Mg)	(In)	(La)	(Si)
Length (l)	n_{ppts}	157	49	81	123	48
	$\bar{x}$ (nm)	230±70	550±190	390±16	550±190	520±180
Thickness (t)	n_{ppts}	69	54	63	65	65
	$\bar{x}$ (nm)	10±3	12±5	10±3	9±3	14±7
Width (w)	n_{ppts}	186	55	63	65	67
	$\bar{x}$ (nm)	29±13	64±31	33±13	32±11	64±31
Aspect Ratio w/t		2.8	5.2	3.3	3.6	2.2
Aspect Ratio l/t		22	45	40	62	38
Volume (nm^3 x 10^4)		6.7	42.7	12.7	15.5	20.8

Table 4. Length of S′ corrugation, y, in specimens aged for 100h at 200°C (y defined in Fig. 1).

Alloy	(Al-Cu-Mg)	(Mg)	(In)	(La)	(Si)
n_{corrug}	105	72	111	170	118
$\bar{y}$ (nm)	93±32	650±360	200±87	300±140	250±110

Table 5. Vickers Hardness after ageing for 100h at 200°C.

Alloy	(Al-Cu-Mg)	(Mg)	(In)	(La)	(Si)
Hardness± 2σ	117 ± 7.2	140 ± 4.7	117 ± 3.0	103 ± 0.8	103 ± 1.9

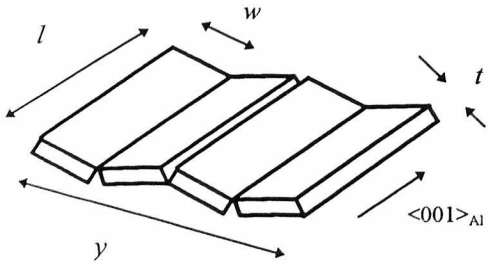

Figure 1. Schematic of the S′ laths and corrugations, indicating the origin of the measurements in Tables 3 and 4.

Figure 2. TEM bright field image, showing the Al-Cu-Mg base alloy after ageing 100h at 200°C. The S′ laths are arranged in corrugated laths, and are seen end-on with the $[001]_{Al}$ imaging condition used.

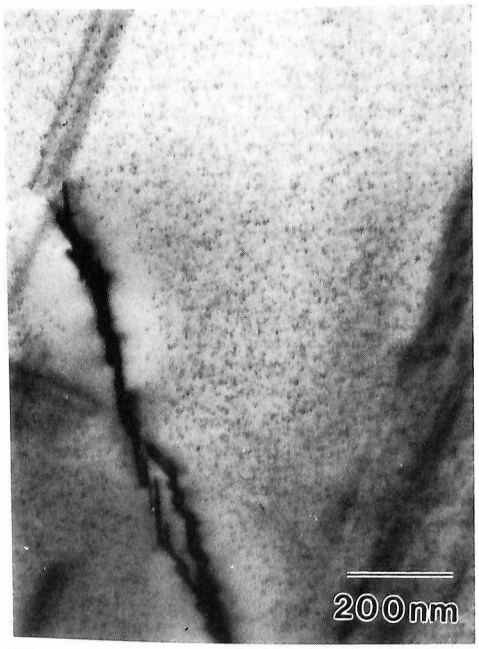

Figure 3. TEM bright field image of the Mg-rich alloy showing the wide spacing of the S′ corrugations and fine GPB zones. B=[001]$_{Al}$.

Figure 4. TEM bright field image showing the In-containing alloy. B=[001]$_{Al}$

Figure 5. TEM bright field micrograph showing the La containing alloy. Note the criss-cross nature of the S′ corrugations and the strain contrast at the precipitate/matrix interface. B=[001]$_{Al}$

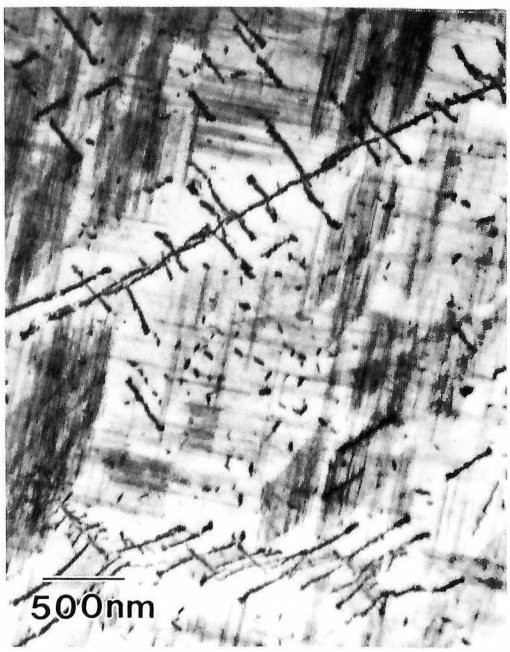

Figure 6. TEM bright field image of the Si-containing alloy, showing the variable precipitate distribution. B=[001]$_{Al}$